Dynamics of Dilute Polymer Solutions at the Final Stages of Capillary Thinning

Andrey Subbotin, Alexander Semenov

Dynamics of dilute polymer solutions at the final stages of capillary thinning

Andrey V. Subbotin[1,2] and Alexander N. Semenov[3]

[1]*A.V. Topchiev Institute of Petrochemical Synthesis, Russian Academy of Sciences, Leninskii prosp. 29, Moscow, 119991, Russia*

[2]*A.N. Frumkin Institute of Physical Chemistry and Electrochemistry, Russian Academy of Sciences, Leninskii prosp. 31, Moscow, 119071, Russia*

[3]*Institut Charles Sadron, CNRS-UPR 22, Universite de Strasbourg, 23 rue du Loess, BP 84047, 67034 Strasbourg Cedex 2, France*

For Table of Contents Use Only

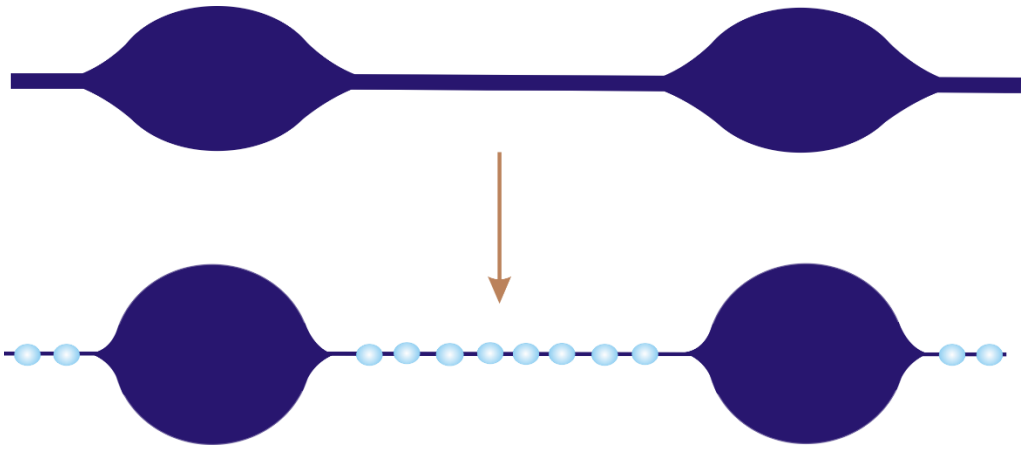

Abstract:

The dynamics of capillary break-up of a fluid thread of a dilute polymer solution near the Θ-point is studied using a molecular approach. Several regimes arising during the development of capillary instability have been identified and investigated. We show that in the course of thread thinning the macromolecules can undergo a coil-stretch transition and analyze its kinetics. In the process of chain stretching, the inertial regime turns into a viscoelastic stage and then a highly viscous quasi-Newtonian regime with almost completely stretched macromolecules. In the viscoelastic regime the hydrodynamic friction force is proportional to the chain extension, and the radius of the thread decreases according to a power law. This differs from the experimentally observed exponential law arising from the linear dependence of the friction force on the contour length of the chain. A possible physical mechanism giving rise to an exponential thinning of the thread formed by dilute polymer solution is discussed. We further established that once the thread radius becomes smaller than the chain contour length after the end of the viscoelastic regime, such ultrafine thread becomes unstable with respect to the development of annular solvent droplets. It is predicted that formation of the droplets occurs with no energy barrier, so a "beads-on-string" structure emerges readily as a result.

I. INTRODUCTION

The dynamics of polymer jets is one of the important areas of polymer rheology with long history of development, which continues to attract a significant scientific interest due to widespread use of such jets for spinning fibers, printing and spraying.[1-3] The property of polymers to form fibers is well known in living nature and is associated with the ability of polymer solutions and melts to undergo large elastic deformations. This process is usually

associated with the transition of macromolecules from coiled to stretched state. However, many aspects of jet thinning and fiber formation still remain poorly understood. Importantly, the jet behavior is often accompanied with various types of instabilities.[4-7]

A noticeable progress has been achieved in the study of flows of Newtonian fluids with a free surface.[8-19] To some extent it can serve as a basis to study also the liquid bridges and jets formed by polymer solutions. The dynamical behavior of a Newtonian fluid thread is related to its Ohnesorge number $\mathrm{Oh} = \eta / \sqrt{\rho \gamma a}$, where a is the radius, ρ is density of the liquid, η is its viscosity and γ is its surface tension. This number reflects the ratio of two timescales, $\tau_I = 2.9\sqrt{\rho a^3 / \gamma}$ and $\tau_V = 6\eta a / \gamma$, which are associated with the Plateau-Rayleigh capillary instability of a thread of radius a and correspond to predominantly inertial and viscous forces, respectively: $\mathrm{Oh} \approx 0.5\tau_V / \tau_I$. If the thread is thick enough so that $\mathrm{Oh} \ll 1$, the inertial and capillary forces dominate (inertia-capillary regime or I-regime) and the radius of the thread neck follows the 2/3 scaling law $a(t) \propto (t_b - t)^{2/3}$,[20] where t_b is the putative breakup time. Otherwise (for $\mathrm{Oh} \gg 1$) the thread behavior is governed primarily by viscous and capillary forces (visco-capillary regime or V-regime) and the neck radius decreases linearly in time, $a(t) \propto (t_b - t)$.[14]

It is well-known that capillary forces constitute a generic mechanism leading to instability of liquid cylindrical threads,[21,22] inherent in both Newtonian and polymer fluids, and to the eventual thread breakup. However, the break-up of a polymer solution string proceeds in a much more complicated way due to viscoelastic behavior. Early experimental[23,24] and theoretical[25,26] studies of pinching-off have revealed an important role of elasticity associated with the transition of polymer chains to an elongated state. Instead of breaking up into individual droplets, a bead-on-string structure is often formed, in which the droplets are connected by long-lived bridges. The emergence of such long-lived bridges depends on the relationship between the longest characteristic relaxation time τ of the quiescent polymer solution and the timescales τ_I and τ_V.

Since the times τ_I and τ_V decrease as the thread gets thinner and τ is constant unfolding of polymer chains must occur at a certain finite diameter of the thread (when $\tau \sim \max(\tau_I, \tau_V)$). During thinning of a thread formed by a solution of high-molecular weight polymers in a low-viscosity solvent, a transition from the inertial-capillary to the elasto-capillary regime can occur even at very low polymer concentrations.[27,28] The theoretical analysis of the elasto-capillary regime was carried out based on a balance of the viscoelastic and capillary forces, while the polymer viscoelasticity was taken into account mainly by using the classical constitutive equations of Maxwell, Oldroyd-B and FENE-P models,[29-35] which are based on a dumbbell model with constant friction. According to these theories the radius of the thread *a* decreases as $a(t) \propto e^{-t/3\tau}$ in the elasto-capillary regime. This exponential law was observed in many experiments with dilute, semi-dilute and concentrated solutions without entanglements,[32-44] in which the methods of CaBER[5,24,35], DoS[40] and ROJER[43,44] rheometry with visualization of pinch-off dynamics were used. The study of extension and breakup of polymer filaments at very high strain rates (high Weissenberg number) was made possible by using a double piston stretching apparatus.[45] At the end of the elasto-capillary (viscoelastic) regime the polymer chains are almost fully elongated, and the polymer solution starts to behave like a quasi-Newtonian liquid of high viscosity associated with the complete stretching of the chains.[33,42] As an important effect it was found experimentally that the apparent relaxation time τ coming from fitting $a(t)$ with an exponential significantly increases with concentration in the dilute solution regime ($c < c^*$). [39,40,46-49] This result is at odds with the Rouse-Zimm theory for dilute solutions, in which the relaxation time depends only on the molecular weight, but not on the concentration. This contradiction triggered questions on how to define a dilute solution and how interchain interactions, including hydrodynamic ones, affect the rheology of solutions in extensional flow.[47-49]

The Plateau-Rayleigh capillary instability was also observed in thin filaments formed by solid gels.[50] As follows from a comparison of elastic and surface energies, the instability arises when the radius of the filament decreases below the length scale $\ell = \gamma / G$ where G is the elastic shear modulus of the solid.[51-53] As a result, two types of morphology have been identified: cylinders on a string and beads on a string.[53]

Another type of instability arising in polymer solution strings is associated with the formation of blistering patterns or pearling patterns at the end of the exponential thinning regime, when the polymer chains are highly stretched,[36,54-60] or with phase separation accompanied by the emergence of small solvent droplets onto the jet surface during a flow-induced extension.[61-63] These types of instabilities differ from the classical Plateau-Rayleigh pinching. Two mechanisms have been proposed to explain this behavior, namely, the migration of macromolecules into thinner regions with a higher concentration due to the stress-concentration coupling effect[64-67] , and the flow-induced phase separation leading to the formation of nano-fibrils, which subsequently condense in the jet core pressing the solvent out to the surface.[68-70] While the first approach uses phenomenological equations for the dynamics of a polymer solution, the second approach is based on molecular concepts. Note that in both cases the instability results in an inhomogeneous distribution of polymer in the jet.

In the present paper we focus on the final stages of capillary thinning of a liquid bridge of dilute polymer solution when the bridge diameter gets smaller than the contour length of macromolecules (section III). Such a regime can also appear in a jet that is stretched under the action of an electric force in the process of electrospinning or under the action of an external force applied to the free end of the jet upon fiber spinning. Recently we studied the behavior of fine threads formed by solutions of rigid rods.[71,72] It has been shown that capillary forces are responsible for the extrusion of the solvent to the surface, where it forms annular droplets, so that the rods are concentrated in the core of the thread (thus leading to the beads-on-string structure). We now extend this theory to the case of thin threads of dilute solutions of long flexible or semi-

flexible macromolecules. It is shown that for aqueous solutions of PEO with $M_w \sim 10^6$ the beaded structure can emerge for the filament thickness of order or below 1μm. Such beads-on-string structures have been indeed observed experimentally[36,38,54-60]. It is noteworthy, however, that it is hard to optically resolve the evolution of these features on a submicron scale, so an improvement of experimental visualization techniques may be required to fully test our predictions.

In the next section II we first discuss the relevant static and dynamical properties the bulk polymer solutions, and then present the basic dynamical equations for capillary thinning of a polymer solution thread. We then turn to the viscoelastic (elasto-capillary) regime associated with the extension-flow induced coil-stretch transition. We show that in dilute theta-solutions the polymer elongation dynamics is strongly affected by hydrodynamic interactions giving rise to a power-law time dependence of the filament radius $a(t) \propto t^{-2}$. Such power law for $a(t)$ was already predicted[44] based on similar ideas. We remind however that most experimental data[33-44,46] rather point to an exponential decay of $a(t)$ even in the dilute solution regime. To tentatively explain this contradiction, we propose a new physical mechanism which can change the thinning law back to the exponential decay (see end of section II). Furthermore, in section V we also discuss a couple of other physical effects which may modify the thinning law rendering it closer to a single-exponential decay.

II. THE DYNAMICS OF POLYMER SOLUTION THREAD

Let us consider a solution of semiflexible macromolecules of contour length L, Kuhn segment length l and diameter d, $d \ll l \ll L$. The number of repeat monomer units in the macromolecules is N, the monomer length equals to $l_1 = L/N$ and the statistical segment length is $b_s = \sqrt{l l_1}$. The equilibrium size of the polymer coils is $R_0 = \sqrt{lL} = b_s \sqrt{N}$. We assume that the concentration of monomer units in solution, c, is less than the coil overlap concentration

$c^* \sim 2N / R_0^3$.[73] For long chains, $N_K \equiv L / l \gg 1$, the condition $c < c^*$ ensures that the polymer volume fraction is small, $\phi = \pi l_1 d^2 c / 4 \ll d / l$, so the solution is isotropic (no tendency for nematic ordering).

The free energy of interactions between polymer segments generally depends on their orientations; per unit volume it is given by[68,69,74]

$$f_{\text{int}} \simeq \frac{T}{2} B c^2 \left(I \left| \ln(1-\phi) \right| / \phi - \Theta / T \right) \qquad (1)$$

where $B = \frac{\pi}{2} l_1^2 d$, $T = k_B T_{abs}$ is temperature in energy units (k_B is the Boltzmann constant), and Θ is the theta-temperature for isotropic dilute solution. The orientational factor $I = \frac{4}{\pi} < \sin\beta >$, where β is the angle between two interacting polymer segments.[74] For the trial orientational distributions defined in eq. 8 of ref. 68 the factor I depends solely on the orientational order parameter $s = \langle \cos\theta \rangle$, where θ is the angle between a polymer segment and the axis of preferred orientation and averaging is performed over the orientations of all segments. The graph of the function $I(s)$ is shown in Figure 1.

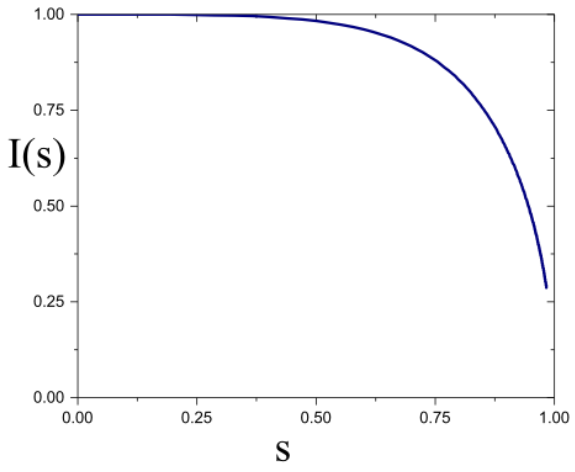

Figure 1. The orientational factor $I(s)$.

We then consider a liquid bridge formed by a drop of the solution placed between two parallel plates and stretched by moving the plates a certain distance apart from each other. After the plate motion is stopped the bridge thickness decreases due to capillary forces. The elongational flow inside the bridge is characterized by the extension rate $\dot{\varepsilon} = \frac{\partial \upsilon_z}{\partial z}$ where υ_z is the flow velocity along the jet axis z. This velocity is connected with the radius of the bridge $a(t,z)$ through the volume conservation equation

$$\frac{\partial a^2}{\partial t} + \frac{\partial}{\partial z}\left(a^2 \upsilon_z\right) = 0 \qquad (2)$$

where it is assumed that v_z is uniform in a cross-section of the jet.

At sufficiently high extension rate $\dot{\varepsilon}$ the chains begin to stretch along the stream. At low concentrations $c < c^*$ a chain stretching is possible if $\dot{\varepsilon}\tau_Z > 1$, where $\tau_Z \sim \eta_s R_0^3 / T$ is the Zimm time.[69,75] The unfolding of the chains in this case occurs as a sharp coil-stretch transition,[68,75] which is accompanied by a significant hysteresis.[48,49] Three polymer solution states of stretched chains can be distinguished. When stretching is not too strong, $R_0 \ll R_z \ll L$, where R_z is the end-to-end distance of the chain along the thread axis, the stretched coils in Θ solvent can be approximated by a cylinder of length $\sim R_z$ and radius $\sim R_0$. The average concentration of monomers inside the stretched coils is $c_{st}(R_z) \sim N / \left(\pi R_0^2 R_z\right)$. It decreases with increasing value of R_z; therefore, for some $R_z = R_z^*$ the coils must begin to overlap. The onset of this regime is defined by the condition $c_{st}^* = c_{st}(R_z^*) \sim c$, leading to $R_z^* \simeq R_0 \frac{\phi^*}{\phi} \simeq \frac{d^2}{4\phi l}$ ($\phi \ll \phi^* \simeq d^2 / \sqrt{l^3 L}$). Thus, at $R_0 \ll R_z \ll R_z^*$ the system can be considered as a dilute solution of extended coils, whereas at $R_z^* \ll R_z \ll L$ the solution of stretched chains is semidilute. When the chains are stretched very strongly, $R_z \sim L$, and the tension force of a chain $\mathcal{T} > T / l$, its transverse

fluctuation size R_n begins to decrease ($R_n < R_0$). The monomer concentration inside the fluctuation volume of such stretched chain, $c_{st} \simeq N/\left(\pi R_n^2 L\right)$, increases as a result, and at $R_n < R_n^* \simeq \left(l_1 c\right)^{-1/2}$ it exceeds the average concentration c, so the extended chains become non-overlapping again: In this regime the average distance between two neighboring chains exceeds R_n, i.e. the polymer solution is similar to a dilute solution of strongly oriented rigid rods.

To study the dynamics of a stretched chain we first assume that there is no flow, $\dot{\varepsilon} = 0$. Then the stretched macromolecule will relax to an equilibrium coiled state and this process can be described using the energy-dissipation balance equation implying that the accumulated elastic energy of a chain transforms into heat (as no external work is done on the system):

$$\frac{dF_{el}}{dt} + \dot{D} = 0 \tag{3}$$

where F_{el} is the elastic free energy of a chain and $\dot{D}$ is the rate of energy dissipation. Introducing the orientational parameter $s = \langle \cos\theta \rangle = R_z / L$, the elastic energy is written as[62,71]

$$F_{el} = \frac{TL}{2l}\left(A\coth A - 1\right), \qquad s = \coth A - 1/A \tag{4a}$$

In what follows we will approximate equation (4a) by

$$F_{el} \simeq \frac{TL}{2l}\frac{s^2\left(3-s^2\right)}{1-s^2} \tag{4b}$$

To find the rate of dissipation $\dot{D}$ first note that the friction force acting on a polymer chain in a flow depends on the chain conformations and interchain interactions.[48] In the dilute solution case the friction force *f* is proportional to R_z (rather than to *N*) due to unscreened hydrodynamic interactions. This idea, which is known as the linear drag model, was proposed long ago[76,77] and further elaborated more recently[48,49] . The reason for such linear dependence ($f \propto R_z$) is that a stretched chain can be considered as a sequence of Pincus blobs (elastic or tension blobs)[75,78] whose volume fraction is always small for $c < c^*$, so the blobs never overlap.

Therefore, the hydrodynamic interactions within a blob are not screened, so a sequence of blobs is hydrodynamically similar to a long rod of length R_z. Next we employ the usual logarithmic approximation for the hydrodynamic drag (cf. Appendix 8.1 of ref. 79). The relative velocity (in z-direction) between a chain segment *n* and the quiescent solvent is $\frac{dR_z}{dt}\left(\frac{n}{N}-\frac{1}{2}\right)$, where $0 \le n \le N$. Therefore, the dissipation function due to polymer/solvent friction is given by

$$\dot{D} = \zeta_{\parallel} \int_0^{R_z} dx \left(\frac{1}{R_z}\frac{dR_z}{dt}\right)^2 \left(x - \frac{R_z}{2}\right)^2 = \frac{\pi}{6}\frac{\eta_s R_z}{k_H}\left(\frac{dR_z}{dt}\right)^2 \tag{5}$$

Here $x = nR_z / N$, $\zeta_{\parallel} = 2\pi\eta_s / k_H$ is the parallel component of the friction coefficient per unit length of the stretched chain, η_s is the solvent viscosity, and k_H is the hydrodynamic factor,[69] $k_H \simeq \ln\left(\xi_H / d\right) \simeq 0.5\ln\left(1/\phi\right)$, where $\xi_H \sim d\phi^{-1/2}$ is the hydrodynamic screening length.[79,80] Substitution of eqs 4b, 5 in eq 3 yields

$$\tau_R \left(1-s^2\right)^2 \frac{ds}{dt} = -1 - \frac{1}{3}\left(s^4 - 2s^2\right) \tag{6}$$

where $\tau_R = \frac{\pi}{18}\frac{\eta_s l L^2}{k_H T}$ is the Rouse relaxation time. This equation gives for $s \ll 1$: $s(t) = s_0 - t/\tau_R$, i.e. the relaxation time of R_z=sL from an initial value $R_{z0} > R_0$ to the equilibrium ($R_z \sim R_0$) is $\tau(R_{z0}) \simeq \tau_R R_{z0} / L$. If $R_{z0} \sim R_0$, we arrive at the Zimm relaxation time $\tau_Z \sim \tau_R / \sqrt{N_K} \sim \frac{\pi}{18}\frac{\eta_s}{T}R_0^3$.[75,77]

The relaxation behavior of macromolecules gets more complex in the presence of a flow whose effect can be taken into account by including the convective term $\left(\dot{s}\right)_{conv} = \dot{\varepsilon} s$ in eqs 6 :[81,82]

$$\tau_R \left(1-s^2\right)^2 \left(\frac{ds}{dt} - \dot{\varepsilon} s\right) = -1 - \frac{1}{3}\left(s^4 - 2s^2\right) \tag{7}$$

Initially the orientational parameter is $s \sim R_0 / L \sim 1/\sqrt{N_K} \ll 1$.

The stresses generated in a polymer solution under flow include contributions from the solvent, $\boldsymbol{\sigma}^s$, and polymer, $\boldsymbol{\sigma}^p$, i.e. $\boldsymbol{\sigma} = \boldsymbol{\sigma}^s + \boldsymbol{\sigma}^p$. In the case of a uniaxial flow with extension rate $\dot{\varepsilon}$ the normal stress difference due to Newtonian solvent is $\sigma_s \equiv \sigma_{zz}^s - \sigma_{rr}^s = 3\eta_s \dot{\varepsilon}$. The polymer component σ_{zz}^p of the stress tensor is determined in the usual way by averaging the product of a polymer chain longitudinal size and the corresponding tension force $f_z = \dfrac{\partial F_{el}}{\partial R_z}$:[79]

$$\sigma_{zz}^p \simeq \frac{c}{N} < R_z f_z > \simeq cT \frac{l_1}{l} \frac{s^2\left(3 - 2s^2 + s^4\right)}{\left(1 - s^2\right)^2} \tag{8}$$

As for the radial component σ_{rr}^p of the polymer stress tensor, it is relatively small, $\sigma_{rr}^p \ll \sigma_{zz}^p$, since the chain size in the radial direction, R_n, is much shorter than its longitudinal size, $R_z \gg R_n$. Therefore, the polymer normal stress difference is $\sigma_p \equiv \sigma_{zz}^p - \sigma_{rr}^p \simeq \sigma_{zz}^p$.

The dynamics of the thread in the scope of the slender body approximation ($\left|\partial a / \partial z\right| \ll 1$) is described by the general momentum equation

$$\frac{\partial}{\partial t}\left(\rho a^2 \upsilon_z\right) + \frac{\partial}{\partial z}\left[a^2\left(\rho \upsilon_z^2 - 3\eta_s \frac{\partial \upsilon_z}{\partial z} - \sigma_p\right)\right] + \gamma a^2 \frac{\partial C}{\partial z} = 0 \tag{9a}$$

Here the radius a and velocity υ_z depend on the axial coordinate z and time t. The total curvature of the thread surface reads

$$C = \frac{1}{a\left(1 + a_z'^2\right)^{1/2}} - \frac{a_{zz}''}{\left(1 + a_z'^2\right)^{3/2}} \tag{9b}$$

so that the Laplace pressure is γC ($a_z' = da/dz$, $a_{zz}'' = d^2a/dz^2$). Based on eqs 7, 8, 9a,b we can describe the dynamics of the thread prior the breakup event. Let us focus on the thinnest part of the bridge (the thread neck of radius $a_{neck} = a$) assuming the dilute solution regime $c < c^*$. If initially $a \gg a^*$ where

$$a^* = \frac{\eta_s^2}{\rho\gamma} \tag{10}$$

is the characteristic length separating inertia dominating and viscosity dominating regimes, the bridge dynamics is determined by the inertial terms in eq 9a. In this regime

$$a = a(t) \sim \left(\gamma / \rho\right)^{1/3} \Delta t^{2/3} \tag{11}$$

where $\Delta t = t_b - t$ is the time left to the breakup (t_b is the breakup time).[15,16] Typically the neck length L_z (defined as the region where the jet radius is close to a_{neck}) is short, $L_z \sim a$, in the inertial regime. With no polymer the thinning law of eq 11 would approximately hold until a becomes smaller than a^* (note that $a^* \sim 10\text{nm}$ for water). The case of polymer solution is different: here the effective viscosity increases due to coil-stretching transition at $\dot{\varepsilon}\tau_Z \sim 1$. From eq 2 we obtain $\dot{\varepsilon}$ in the neck region (where $\partial a / \partial z$ is small and can be neglected):

$$\dot{\varepsilon} \simeq -\frac{2}{a}\frac{da}{dt} \tag{12}$$

Thus, we get using eqs. 11, 12: $\dot{\varepsilon} \simeq \frac{4}{3}\frac{1}{\Delta t}$, leading to $\Delta t \sim \tau_Z \sim \frac{\pi}{18}\frac{\eta_s}{T}R_0^3$ and the critical thread radius a_{cs} at the coil-stretch transition,

$$a_{cs} \sim \left(a^* / l_{\gamma T}^4\right)^{1/3} R_0^2 \tag{13}$$

where $l_{\gamma T} \equiv \sqrt{T/\gamma}$ (note that $l_{\gamma T} \sim 0.2\text{nm}$ for water). Obviously $a_{cs} \gg a^*$ if

$$R_0 \gg \left(a^* l_{\gamma T}^2\right)^{1/3} \tag{14}$$

which means that the polymer chain is long, $N_K \gg 1$. The subsequent flow-induced coil-stretching at $a = a(t) < a_{cs}$ is defined primarily by convection, $dR_z / dt = \dot{\varepsilon} R_z$. Therefore

$$R_z \sim R_0 \left(a_{cs} / a\right)^2 \tag{15}$$

where $a = a(t)$ is still defined in eq 13 for the inertial regime.

It is important, however, that the inertial regime breaks as soon as the normal stress difference, $\sigma_p \equiv \sigma_{zz}^p - \sigma_{rr}^p \simeq \sigma_{zz}^p \sim \frac{3cT}{N}\left(R_z / R_0\right)^2$, becomes comparable to the capillary pressure γ / a (cf. eq 9a). This happens at $a \sim a_v$

$$a_v \sim \left(\frac{c}{c^*}\right)^{1/3} R_0^{5/3} a^{*4/9} l_{\gamma T}^{-10/9} \tag{16}$$

At $a < a_v$ the thread dynamics is defined by a competition of viscoelastic and capillary forces. Neglecting the inertial effects in this regime, the force balance implies that $\sigma_{zz} - \sigma_{rr} \sim \gamma / a$.[73] Furthermore, here we can also neglect the solvent contribution to the total normal stress difference since $a_v \gg a^*$ (which is valid due to the assumed condition, eq 14). This leads to the following important relation

$$\sigma_p \sim \gamma / a \tag{17}$$

Note, that for a Newtonian fluid $\sigma_{zz} - \sigma_{rr} \simeq 3\eta\dot{\varepsilon}$ is typically $\sim 0.425\gamma / a$ in the viscosity-dominated regime (called the viscous regime in ref. 17).[83] Remarkably, the purely convective stretching, eq 15, can not work in this new *viscoelastic* regime (at $a < a_v$): otherwise the balance between σ_p and γ / a would be destroyed. Moreover, the "inertial" eq 11 for thread thinning also fails in this regime.

To obtain both $a(t)$ and $R_z(t)$ here we use eqs 7, 8, 12, 17 in the regime $s \ll 1$ (assuming that the chains are far from the full extension, $R_z \ll L$). Eqs 7, 8 can be simplified as

$$\frac{dR_z}{dt} \simeq \dot{\varepsilon} R_z - \frac{L}{\tau_R} \tag{18}$$

$$\sigma_p \simeq 3\frac{cT}{N}\left(R_z / R_0\right)^2 \tag{19}$$

Solving these equations, we find

$$R_z \sim \frac{L}{3}\left(t/\tau_R\right), \quad a \sim a_0\left(\tau_R/t\right)^2, \quad \dot{\varepsilon} \simeq 4/t, \qquad t \le \tau_R \tag{20}$$

where

$$a_0 = \frac{3}{2}\frac{c^*}{c}\left(l/l_{\gamma T}\right)^2 R_0 = \frac{3\pi}{4}\frac{\gamma l d^2}{\phi T}. \tag{21}$$

is independent of molecular weight $M_w \propto L$. In fact, a_0 is defined by the relation $\dot{\varepsilon}\tau_R \sim 1$ where $\tau_R \propto M_w^2$ and the thinning time $1/\dot{\varepsilon} \sim \tau_V \sim \eta a_0/\gamma$ is proportional to the effective viscosity η which, in turn, also scales as M_w^2 in the stretched-chain regime, $R_z \sim L$ (see eq below). The 2 effects thus compensate each other yielding an M_w -independent a_0. On the other hand, the viscosity due to highly stretched chains is proportional to their concentration, $\eta \propto \phi$, hence $a_0 \propto 1/\phi$ since τ_R is virtually independent of ϕ. It is therefore found that the thread thinning follows a power law, $a = \kappa t^{-2}$, where the prefactor κ is inversely proportional to the polymer concentration and depends on the polymer chain parameters. Importantly, the prefactor does not depend on the initial radius of the thread. Hence, as soon as the bridge enters the viscoelastic regime, it must become nearly uniform over a long axial segment (with $a(t,z) \approx a_{neck}(t)$), which is in agreement with experimental results.[39,46,47] Noteworthily, the 3 scaling dependences in eq. (20) are in full agreement with the results of a detailed theoretical study[48] (cf. eq. 57 in ref. 48 and the text below it) taking into account a partial screening of hydrodynamic interactions in dilute solutions (this screening, however, is weak and leads to just logarithmic corrections to the scaling laws).

The power law $a \propto t^{-2}$ arises due to a linear dependence of the friction force on the longitudinal size of the chains. This behavior is a consequence of hydrodynamic interactions which should prevail for low polymer volume fraction $\phi \ll \phi^*$. It clearly differs from the exponential thinning law typically observed in experiments with polymer solution threads. Such an exponential behavior, which is not expected for dilute solutions according to our theory, can

be explained by the following physical effect: When the stretched chains are in a semidilute regime there are contacts between monomers of different chains. If we assume that the monomers (or a group of monomers) can form transient bonds between the chains, so that the lifetime τ_b of a bond is long, $\tau_b \gg \eta_s d^3 / T$, then the polymer chain dynamics can change drastically[84]: in this case it can become Rouse-like with a high effective friction per chain, ζ^*, which is proportional to the bond lifetime and the number of bonds n_b. The bond number per chain is $n_b \sim \phi N$, i.e. it is proportional to the number of monomers, therefore the chain relaxation time $\tau_R^* \sim \tau_b \phi^2 N^2 \gg \tau_R$ and eq (18) should be replaced by the Rouse type equation $\frac{dR_z}{dt} = \dot{\varepsilon} R_z - \frac{R_z}{\tau_R^*}$. The joint solution of this equation and eqs (8), (12), (19) leads to exponential thinning of the thread, $a \propto \exp\left(-\frac{2t}{3\tau_R^*}\right)$. For consistency with thermodynamic polymer solubility, we have to demand that these bonds are difficult to dissociate, but also equally difficult to create, so that the statistical weight of a bond is similar to that of a simple contact. The increase of the relaxation time τ_R^* with the polymer concentration is in qualitative agreement with the experiment; however, experimentally, a weaker dependence is observed.[35,38,39,42,46,47] Such bonds are possible, for example, in PEO/water systems which are often used in experiments. They originate from attractive hydrophobic interactions of CH_2 groups in PEO, and by hydrogen bonding between PEO units mediated by water molecules.[85] These interactions lead to the well-known phenomenon of clustering in aqueous PEO solutions.[86] Such reversible bonds may be also expected in aqueous solutions of polyacrylamide (PAM).[33,34] They can also lead to formation of microscopic strands, which are responsible for significant non-Newtonian effects in dilute polymer solutions during extension.[87] Thus, the thinning behavior of filaments of a polymer solution generally depends on the chemical nature of the chains, their concentration, and interchain interactions, which are affected by the extension flow.

Note however that our approach based on the hydrodynamic description is quite general and does not rely on the chemical nature of macromolecules.

Noteworthily, deviations from the exponential thinning law in very dilute solutions have been observed experimentally,[39,46,47] for example, in aqueous PEO solutions (M_w=10^6 g/mol) with concentration $c \leq 0.03$ wt % < $c^* = 0.17$ wt %.[38] As far as we know a detailed analysis of the thinning law for jets of very dilute polymer solutions has not yet been performed experimentally. (In our opinion the experimentally probed viscoelastic regime which spans only about a half of an order of magnitude in time is insufficient to unambiguously distinguish between the exponential and the power law of jet thinning – cf. Figs. 2,5 in ref. 46).

Note that a_0 is larger than the Gaussian coil size R_0 since typically $l > l_{\gamma T}$ and $c \leq c^*$. On the other hand, a_0 is smaller than the total chain length L if $c/c^* > (l/l_{\gamma T})^2 N_K^{-1/2}$, i.e. $c > c_{\min}$, where the minimum concentration

$$c_{\min} \sim \frac{1}{N}\frac{l}{l_1^2 l_{\gamma T}^2} = 1/(N_K l_1 l_{\gamma T}^2) \tag{22}$$

corresponds to a really dilute regime, $c_{\min} << c^*$ for $N_K >> 1$. For example, the value of a_0 for PEO/water solution is $a_0 \simeq 6\text{nm}\cdot(1/\phi)$ ($l \approx 0.8\text{nm}$, $l/d \approx 2$, $\gamma \approx 73\text{mN/m}$), for PAN/DMSO solution $a_0 \simeq 17\text{nm}\cdot(1/\phi)$ ($l \approx 2.5\text{nm}$, $l/d \approx 5$, $\gamma \approx 46\text{mN/m}$), and for DNA/water solution $a_0 \simeq 10\mu\text{m}\cdot(1/\phi)$ ($l \approx 100\text{nm}$, $l/d \approx 20$, $\gamma \approx 73\text{mN/m}$). Therefore, a_0 ~ 1μm for dilute solutions ($\phi \leq 1\%$) of flexible polymers (PEO, PAN), and it is much larger for semirigid polymers like DNA.

At longer times $t > \tau_R$ the polymer chains become nearly fully stretched, $R_z \sim L$, and the bridge enters the 'final' stage of capillary thinning, which proceeds according to the classical law:[33,34]

$$a \sim \frac{\gamma}{6\eta}\Delta t, \qquad a < a_0 \tag{23}$$

with a renormalized viscosity[62,71,77]

$$\eta \simeq \eta_s \left(1 + \frac{\pi}{18 k_H} \frac{c}{N} R_z^3 \right) \tag{24}$$

where the second term dominates (i.e., we assume $c \gg N / L^3 \sim c^* / N_K^{3/2}$, which is compatible with $c \ll c^*$). Note, that eqs 23, 24 can be derived based on eqs 8, 9, 17, and that $a \sim a_0$ corresponds to $\Delta t \sim \tau_R$. Note also that – from the polymer stress point of view – the extended chains behave as rigid rods of the same length in the 'final' regime, $a < a_0$. Based on the above results, in Figure 2a we present a schematic evolution of the thread (neck) radius, in which inertial-capillary, viscoelastic and high-viscosity regime are identified.

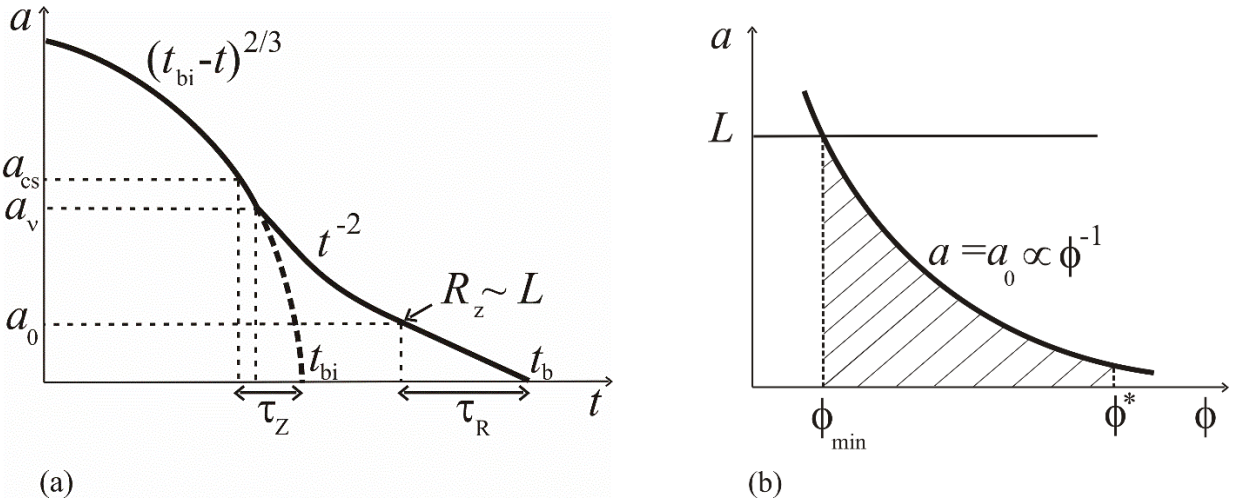

Figure 2. (a) Schematic plot of the thread radius evolution in which 3 main stages are identified, namely the inertia-capillary regime, $a(t) \propto \left(t_{bi} - t \right)^{2/3}$ where t_{bi} is the inertial breaking time, the viscoelastic regime, $a(t) \propto 1/t^2$, and the highly viscous regime, $a(t) \propto \left(t_b - t \right)$. (b) Diagram in coordinates (ϕ, a) showing the region of droplet formation in the highly viscous regime (shaded area). Here $\phi_{\min} \propto 1/L$ is the minimum volume fraction and $\phi^* \propto 1/\sqrt{L}$ is the coil overlap volume fraction.

Let us turn to analysis of a polymer string in which the formation of interchain transient bonds is the dominant friction mechanism. In this case the transition from the regime with exponential thinning to the quasi-Newtonian regime occurs at the radius of the thread a_0, which is determined from the condition $\gamma / a_0 \sim \eta\dot{\varepsilon}$, where $\eta \sim \eta_s \phi N^2$ is the renormalized viscosity (see eq 24) and $\dot{\varepsilon} \sim 1/\tau_R^* \sim \left(\tau_b \phi^2 N^2\right)^{-1}$. From here we find $a_0 \sim \gamma \tau_b \phi / \eta_s$. It is interesting to note that this radius is independent of the number of monomers in the chain.

In the next section we focus on the thread dynamics in the high-viscosity regime where the basic characteristic timescale of thread thinning is defined by τ_R or τ_R^*.

III. JET INSTABILITY AND EMERGENCE OF ANNULAR SOLVENT DROPLETS

Let us consider the mid-part of the bridge in the 'final' regime, where the bridge is thin ($a \le a_0 \ll L$, Figure 2b) and rather uniform axially (so, it can be approximated as a cylinder). As shown above the chains are stretched almost completely along the thread axis. The number of chains in the cross-section is

$$m_0 \sim \pi a^2 L c / N \sim \frac{9\pi}{2} \frac{c^*}{c} \frac{b_s l^3}{l_{\gamma T}^4} N^{1/2} \tag{25}$$

for $a \sim a_0$ (b_s is statistical segment). This number is large both for $c \sim c^*$ and $c \ll c^*$ since $N \gg 1$. As already mentioned, the strongly stretched polymer chains seem to be rheologically equivalent to rodlike macromolecules. Assuming this equivalence one can try to describe the late stages of thread thinning using the results for solutions of rigid rods[71,72] showing that the thread in the regime $a \ll L$ can get unstable with respect to solvent release in the form of annular droplets. It is important to note, however, that in the case of rodlike macromolecules the droplets

can not emerge spontaneously: their formation is an activated process taking place if the polymeric osmotic pressure is much weaker than the capillary pressure, $\Pi_0 \ll \gamma / a$. In the case of semiflexible polymers the osmotic pressure in the solution is[70,72]

$$\Pi \simeq cT\left[\frac{1}{N}+\frac{1}{2}Bc\left(\frac{I(s)}{1-\phi}-\frac{\Theta}{T}\right)\right] \tag{26}$$

Here the first term in brackets is due to translational energy and the second term is due to interactions (B -is the second virial coefficient, see eq 1). In what follows we will assume that the system is close to the Θ-point, i.e. $1-\Theta/T \ll 1$ and $k+\phi > 0$, where $k \equiv I(s)-\Theta/T$ ($|k| \ll 1$). Hence, for $1/N \ll \phi \ll d/l$ and $a \le a_0$, $p \equiv \Pi\, a/\gamma \le 3(k+\phi)\phi\, l/d + 3l/L \ll 1$.

The activation energy of an annular solvent droplet in the case of rods has been calculated in refs. 71,72. The activation state for a droplet nucleation involves a finite deformation of the cylindrical thread adopting a slightly perturbed axially symmetric shape with radius $a = a(z)$ weakly deviating from the mean radius a_m (equal to the thread radius far from the droplet): $|a - a_m| \ll a_m$ (see Figure 3a).

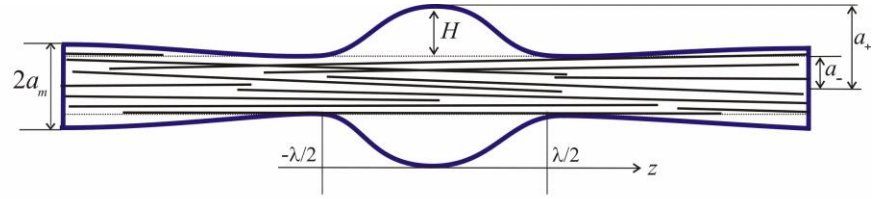

(a)

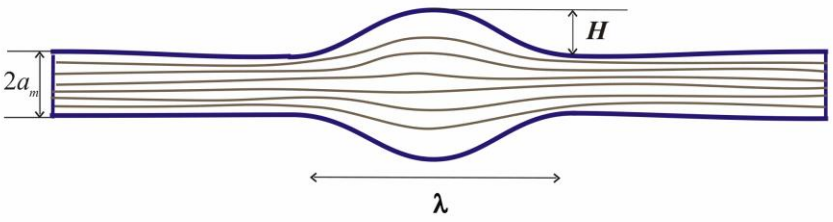

(b)

Figure 3. (a) Thread deformation for a solution of rodlike macromolecules. $H = a_+ - a_-$ is the annular droplet height, λ is its length along the axis. (b) Illustration of the thread structure with a single annular solvent droplet for a solution of semiflexible chains involving their bending and partial penetration into the droplet. The characteristic length of the annulus is $\lambda \sim 2\pi a_m$ and its thickness is H.

The annular droplet of solvent is located in the region $-\lambda/2 \le z \le \lambda/2$ (λ is the droplet length, $a_m < \lambda \ll L$). The rods are confined inside the core of radius $a_{core}(z)$ ($a_{core}(z) = a(z)$ outside the droplet region, $|z| > \lambda/2$, and $a_{core}(z) = a_-$ for $|z| \le \lambda/2$). The optimum shape of the droplet is found by minimization of the excess surface area $A_d = 2\pi \int_{-\lambda/2}^{\lambda/2} a(z)\sqrt{1+a_z'^2}\,dz - 2\pi\lambda a_-$ at the fixed core radius a_- and droplet volume $V_d = \pi \int_{-\lambda/2}^{\lambda/2} a^2(z)dz - \pi\lambda a_-^2$. It corresponds to a surface of a constant curvature C, defined by the differential equation

$$a_+ a_- + a^2 = \frac{2a}{C\sqrt{1+a_z'^2}}, \qquad a_+ + a_- = 2/C \tag{27}$$

where $a = a(z)$, $a_- \simeq a_m$ is the jet radius outside the droplet region, and a_+ defines the height (thickness) H of the solvent droplet: $H = a_+ - a_-$. Equation (27) follows from eq (9b) upon integration. Thus, the total curvature of the droplet surface is $C = \frac{1}{a_-}\left(1+\frac{H}{2a_-}\right)^{-1}$. For weak perturbations, $H \ll a_m$, the length λ, the surface area A_d and the volume V_d of the annular droplet are found by solving eq 27 and can be written as expansions for small H/a_m

$$\lambda \simeq 2\pi a_m\left(1-\frac{H}{2a_m}\right), \qquad A_d \simeq 4\pi^2 a_m^2\left(1-\frac{H}{a_m}\right), \qquad V_d \simeq 2\pi^2 a_m^2 H\left(1+\frac{3H}{2a_m}\right) \tag{28}$$

The total curvature of the droplet can be represented as

$$C \simeq \frac{1}{a_m} - \frac{V_d}{\left(2\pi a_m^2\right)^2} \tag{29}$$

The free energy changes as the solvent is squeezed from the thread core to the surface forming a droplet of volume V_d. The total free energy change (minimal work required to form the droplet) is represented as a sum of osmotic and capillary terms $\Delta\mathcal{F} \simeq \Delta\mathcal{F}_\Pi + \Delta\mathcal{F}_{surf}$. The osmotic increment can be found from $d(\Delta\mathcal{F}_\Pi) = \Pi dV_d$. During the process the local concentration of polymer in the thread core changes only slightly, so the osmotic pressure is nearly constant, $\Pi \simeq \Pi_0$, so $\Delta\mathcal{F}_\Pi \simeq \Pi_0 V_d$. The surface energy $\Delta\mathcal{F}_{surf}$ varies with V_d as $d\left(\Delta\mathcal{F}_{surf}\right) = \gamma\Delta C \cdot dV_d$, where $\Delta C = C - 1/a_m$, therefore

$$\Delta\mathcal{F}_{surf} \simeq -\pi^2\gamma H^2 / 2 \tag{30}$$

and

$$\Delta\mathcal{F} \simeq \Pi_0 V_d - \frac{\gamma V_d^2}{2\left(2\pi a_m^2\right)^2} \tag{31}$$

The energy $\Delta\mathcal{F}\left(V_d\right)$ shows a maximum at

$$V_d = V_d^* = \left(2\pi a_m^2\right)^2 \Pi_0 / \gamma \tag{32}$$

which corresponds to the activation energy

$$F_{bar} \simeq 2\pi^2 a_m^4 \Pi_0^2 / \gamma \tag{33}$$

The analysis given in refs. 71, 72 shows that the nucleation energy barrier F_{bar} can stay high ($F_{bar} \gg T$) even for $a_m \ll L$ leading to a very low droplet nucleation rate unless the thread radius falls below a threshold a_c: $a_m < a_c \ll L$. It is shown below that the latter condition is irrelevant for the case of (semi-)flexible chains.

In fact, there is a significant difference between the droplet formation process for rod-like macromolecules and flexible chains: while rigid rods have to stay inside the cylindrical core, the

chains may bend and (at least partially) penetrate into the emerging annular droplet, Figure 3b. The driving force for such penetration is of osmotic nature. It is opposed by the bending force due to chain tension $\mathcal{T}$. In turn $\mathcal{T}$ is maintained by the extensional flow which keeps the chains in the stretched state:

$$\mathcal{T} \sim \zeta_{\|} \dot{\varepsilon} L^2 \sim \frac{\gamma}{a} \left(c l_1 \right)^{-1} \tag{34}$$

(cf. section III; $\dot{\varepsilon} \sim 1/\Delta t \sim 1/\tau_R$ for $a \sim a_0$). The above equations gives $\mathcal{T} \sim T/l$ for $a \sim a_0$, as it should be since at $a \sim a_0$ the chains are stretched almost completely (with $s \sim 0.5$), so the stretching energy per Kuhn segment is $\sim T$. (Note that $s=R_z/L$ can be considered as the degree of stretching.) The bending force per unit length along the chain is

$$f_{\perp} = \mathcal{T} C$$

where C is now the chain curvature. The force $f_{\perp}$ is oriented perpendicular to the chain (that is, in the radial direction). The coarse-grained chain trajectory can be defined as

$$r = r_0 + h(r_0, z)$$

where r_0 is the distance between the chain and the jet axis far away from the droplet region ($|z| \gg a$). For weak deformation, $\left|\frac{\partial h}{\partial z}\right| \ll 1$, the curvature $C \simeq \frac{\partial^2 h}{\partial z^2}$, and the bending force per unit volume is

$$F_{bend} = c l_1 f_{\perp} = \mathcal{T} c l_1 \frac{\partial^2 h}{\partial z^2} \sim \frac{\gamma}{a} \frac{\partial^2 h}{\partial z^2} \tag{35}$$

Let us turn to the osmotic force. The local osmotic pressure increment is

$$\delta \Pi \simeq T \upsilon^* c_0 \delta c \tag{36}$$

where c_0 is the mean concentration far from the droplet region, δc is the local concentration increment, $|\delta c| \ll c_0$, and

$$\upsilon^* = \frac{1}{Tc_0}\left(\frac{\partial \Pi}{\partial c}\right)_T \qquad \text{at} \quad c = c_0 \tag{37}$$

Using eq 24 and neglecting the ideal-gas pressure, υ^* can be estimated as

$$\upsilon^* \sim dl_1^2\left(k+\phi\right) \ll dl_1^2 \tag{38}$$

The system gets diluted if h increases with r:

$$\delta c / c_0 \simeq -\partial h / \partial r \tag{39}$$

where we assumed that $h \ll r$, so that $r = r_0 + h$ is always close to r_0 and $\left|\delta c\right| \ll c_0$. The osmotic force (per unit volume) in the radial direction reads (on using eqs 36, 39)

$$F_{osm} \simeq -\frac{\partial \Pi}{\partial r} \simeq k_\Pi \frac{\partial^2 h}{\partial r^2} \tag{40}$$

where

$$k_\Pi = T\upsilon^* c_0^2 \tag{41}$$

The force balance, $F_{bend} = F_{osm}$, then gives

$$\frac{\gamma}{a}\frac{\partial^2 h}{\partial z^2} + k_\Pi \frac{\partial^2 h}{\partial r^2} = 0 \tag{42}$$

This linear elliptic equation must be supplemented by the boundary condition $h(a_m, z) = h_m(z)$, where $h_m(z) = a(z) - a_m$. It can be easily solved using the Fourier transform for *z* variable. For a perturbation $h_m(z)$ localized within $\left|z\right| \le \lambda/2$ (for example $h_m(z) \sim h_m(0)\left[1+\cos(qz)\right]$ with $q = 2\pi/\lambda$) we get

$$h(r_0, z) \sim h_m(z) e^{-(a_0 - r_0)/l_r} \tag{43}$$

where $l_r^2 \sim k_\Pi\left(a/\gamma\right)q^{-2}$, $q \sim 1/a$ (recall that $\lambda \sim 2\pi a$, cf. eq 28), so

$$l_r \sim a\alpha\,, \qquad \alpha \equiv \sqrt{k_\Pi\left(a/\gamma\right)} \tag{44}$$

Eq 43 is applicable if $l_r \ll a$, i.e. $\alpha \ll 1$. It means that the polymer concentration is perturbed in a narrow skin-zone of thickness $\sim l_r$. The condition $|\delta c| \ll c_0$ in this zone is satisfied if $h_{\max} \equiv h_m(0) \ll l_r$ since $\delta c / c_0 \sim -h_m / l_r$. In this case the total (bending and osmotic) polymer deformation energy $\mathcal{F}_{def}$ is

$$\mathcal{F}_{def} \sim \gamma \alpha h_{\max}^2 \tag{45}$$

It should be compared with the capillary energy gain (cf. eq 28):

$$\mathcal{F}_{cap} = -\Delta \mathcal{F}_{surf} \simeq \frac{\pi^2}{2} \gamma H^2 \tag{46}$$

Here H is the undulation amplitude (cf. Figure 2b), $H \geq h_{\max}$. It is therefore clear that for $\alpha < const \sim 1$ the deformation energy is subdominant, so the droplet formation is favorable and occurs *without any energy barrier*. This condition is corroborated by the following argument: for $h_{\max} \sim l_r$ the concentration decrement at the polymer core boundary, $r = a_m + h_m(z)$, is comparable to c_0, so the total concentration tend to vanish in this regime. The condition $c = 0$ obviously means that polymer chains can not move further into the solvent droplet, in other words this condition defines the boundary of the polymer accessible zone (core/solvent interface, cf. Figure 2b). Therefore $h_{\max}$ can not significantly exceed l_r ($h_{\max} \sim l_r$), so the polymer deformation energy cannot increase any more once the droplet grows beyond $H \sim l_r$. As a result, the total energy $\mathcal{F}_{cap} + \mathcal{F}_{def}$ keeps decreasing also in the regime $H \gg l_r$.

To resume, we established the following condition of spontaneous droplet formation (cf. eqs 41, 44):

$$\alpha^2 = T \upsilon^* c_0^2 \left(a / \gamma \right) < const \sim 1 \tag{47}$$

Let us verify the above condition for $a \sim a_0$. Taking into account eqs 19, 37 we get

$$\alpha^2 \ll \phi l / d \ll 1 \tag{48}$$

Therefore the condition (47) is always valid in the extended chain regime, $a \le a_0$ (recall the condition $\phi \ll d/l$ established at the beginning of section II). In other words, the spontaneous droplet formation is predicted to start as soon as the chains become strongly extended. At that point many droplets can grow simultaneously with a minimal separation $\lambda \sim 2\pi a_0$.

Since the formation of droplets occurs without a barrier, it is of interest to obtain the dispersion relation and to identify the fastest growing mode. This is done below using the volume conservation equation (2) and the momentum equation (9a), where we neglect the contribution of the solvent viscous stress and inertial forces (which are weaker than capillary forces). The average number of chains in a cross-section of the filament is $m_0 \sim \pi a_0^2 Lc/N$. Assuming that the chains do not move along z-axis (since they are strongly stretched and the wave-length $\lambda << L$) and taking into account that the friction force per unit length of the thread is $\zeta_{\|} m_0 \upsilon_z$ the momentum equation is written as

$$\zeta_{\|} m_0 \upsilon_z + \gamma a^2 \frac{\partial C}{\partial z} = 0 \tag{49}$$

Here we omitted the viscous term $\sim \eta_s v_z a^2/\lambda^2 \ll \zeta_{\|} m_0 v_z$; it is negligible since $\lambda > a$ and $m_0 \gg 1$. Using the relevant formula for the total curvature $C \simeq \frac{1}{a} - \frac{\partial^2 a}{\partial z^2}$ and performing the linear stability analysis assuming $a - a_0 = \varepsilon_1 e^{\Gamma t + iqz}$, $\upsilon_z = \varepsilon_2 e^{\Gamma t + iqz}$ where $q=2\pi/\lambda$ and $\varepsilon_1, \varepsilon_2$ are small amplitudes of perturbations one finds the dispersion relation:

$$\Gamma = \frac{\gamma}{a_0 \zeta_{\|} m_0} \left(q\, a_0\right)^2 \left(1 - \left(q\, a_0\right)^2\right) \tag{50}$$

It leads to the following characteristics of the fastest-growing mode

$$q^* = \frac{1}{a_0\sqrt{2}}, \qquad \Gamma^* = \frac{\gamma}{a_0 \zeta_{\|} m_0} \left(q^* a_0\right)^2 \left(1 - \left(q^* a_0\right)^2\right) \tag{51}$$

It is interesting to note that the period λ of the fastest growing mode coincides with the similar period for an inviscid liquid even if the friction is large. Thus, the period of the growing structure is $\lambda^* \simeq 2\pi\sqrt{2}a_0 \sim 2\pi a_0$. The characteristic growth time is $1/\Gamma^* \sim \frac{\zeta_{\|} m_0 a_0}{\gamma}$.

The droplet formation time can also be estimated by considering a gradual growth of a single solvent annulus of thickness $H = H(t)$, $H \ll a_0$, and volume $V(t) \simeq 2\pi^2 a_0^2 H(t)$ around the thread core (cf. eq. 28). The growth kinetics of the droplet volume is governed by the following equation

$$\frac{dV}{dt} = 2J \tag{52}$$

where $J \simeq \pi a_0^2 \upsilon$ is the solvent current through the thread cross-section, factor 2 means that the liquid enters the droplet from both sides and υ is the solvent axial velocity in the thread core near the droplet (at $z = \pm\lambda/2$). Using eq 52 we get $\upsilon \simeq \pi dH(t)/dt$. The rate-of-change of the droplet height $H(t)$ can be found using the energy-dissipation balance equation:

$$\frac{d\,\Delta\mathcal{F}_{surf}}{dt} + \dot{\mathcal{D}} = 0 \tag{53}$$

where $\Delta\mathcal{F}_{surf}$ is defined in eq 30, and we neglected the subdominant polymer deformation energy (cf. eq 45) since $\alpha \ll 1$ (cf. eq 48). The total rate of energy dissipation, $\dot{\mathcal{D}}$, arises due to friction between solvent and polymer segments in the jet section of length $\sim\lambda$ around the droplet. It reads

$$\dot{\mathcal{D}} \simeq \pi a_0^2 c_0 l_1 \zeta_{\|} \lambda \upsilon^2 \simeq m_0 \zeta_{\|} \lambda \upsilon^2 \tag{54}$$

where m_0 is defined in eq 25. Using eqs 30, 53, 54 we find the linearized master equation for the droplet height:

$$\frac{dH}{dt} = \frac{1}{\tau^*} H \tag{55}$$

where the characteristic time τ^* is

$$\tau^* = \frac{m_0 \zeta_{\|} \lambda}{\gamma} \sim \frac{\eta_s \phi}{\gamma d^2} a_0^3 \tag{56}$$

Note that τ^*, eq 56, agrees with $1/\Gamma^* \sim \frac{\zeta_{\|} m_0 a_0}{\gamma}$ estimated below eq 51. Thus, the droplet height grows nearly exponentially

$$H(t) = h_0 \exp(t/\tau^*) \tag{57}$$

where h_0 is the initial amplitude. The time $\tau^* \sim \Gamma^{-1}$ is much shorter than both the Rouse time τ_R and the thread thinning time $\sim 6a\eta/\gamma$, which (for $a \sim a_0$) is comparable to τ_R:

$\tau^*/\tau_R \sim (a_0/L)^2 \ll 1$ if $c \gg c_{\min}$ (cf. eq 23).

IV. THE FINAL STAGE OF DROPLETS GROWTH

The exponential growth of the droplets ends up when the height H becomes comparable with a_0 defined in eq 21 (note that, as shown in the previous section, the initial thread radius at the onset of the growth process is $a \sim a_0$). At this point roughly half of the solvent is already squeezed into the droplets while another half remains in the polymer strings connecting the droplets. The core thinning driven by the capillary forces continues in the nonlinear regime (where $a \ll a_0$ and $\frac{d \ln H}{dt}$ depends on time) which is considered below. The thinning of a string stops when the capillary pressure becomes equal to the osmotic pressure Π defined in eq 26:

$$\frac{\gamma}{a} = \Pi \simeq \frac{4}{\pi} \frac{T}{d^3} (k + \phi) \phi^2 \tag{58}$$

(here we neglected the ideal-gas pressure and assumed that ϕ<<1; a is the string radius). Taking into account that in the nonlinear regime $\phi = \phi_0 a_0^2 / a^2$ and $\phi \gg k + \phi_0$, where ϕ_0 is the initial polymer concentration before the droplet formation, we arrive at the following maximum polymer volume fraction in the string ϕ_∞:

$$\phi_\infty^{5/2} \simeq \beta, \qquad \beta \equiv \frac{\pi}{4} \frac{\gamma d^3}{T a_0 \sqrt{\phi_0}} \tag{59}$$

Recalling that a_0 is defined in eq 21, we find that $\beta \sim \sqrt{\phi_0}\,(d/l) \ll 1$ and

$$\phi_\infty \simeq \beta^{2/5}, \qquad a_\infty \simeq a_0 \sqrt{\phi_0}\, \beta^{-1/5} \tag{60}$$

where a_∞ is the minimum string radius and $\sqrt{\phi_0}\,\beta^{-1/5} \simeq \left(\phi_0^2 l / d\right)^{1/5} << 1$.

In the regime of thin polymer strings ($a(t) \ll a_0$) the characteristic size H of solvent droplets is much larger than the string thickness, $H \gg a$, hence the droplets are nearly spherical with radius $R \simeq H \sim a_0$. As a result, the droplet capillary pressure, γ / R, can be neglected in comparison with the capillary pressure in the strings, $P_{cap} = \gamma / a$. The droplets are connected by string segments of length Λ (Λ-string) which is found from the volume conservation $\pi a_0^2 (\Lambda + 2R) = (4\pi/3) R^3 + \pi a^2 \Lambda$, i.e., $\Lambda \sim a_0$ for $R \sim a_0$ (Figure 4).

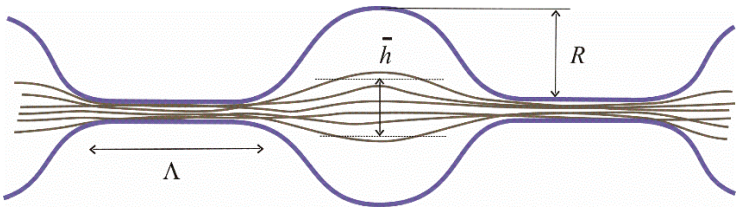

Figure 4: Illustration of a beads-on-string structure involving partial penetration of the macromolecules into the droplets of radius *R*. $\bar{h}$ is the characteristic lateral size of the penetration zone and Λ is the characteristic length of the strings.

In the transient regime, $a_\infty < a \ll a_0$, a high pressure P_{cap} inside a Λ-string generates the solvent flow towards its ends leading to the string thinning due to extensional solvent flow with rate $\dot{\varepsilon} = -\frac{2}{a}\frac{da}{dt}$. The solvent velocity $\upsilon = \upsilon(x,t)$ along the string $(0 < x < \Lambda)$ is $\upsilon \simeq \frac{\dot{\varepsilon}}{1-\phi}\left(x - \Lambda/2\right)$.[72] The rate $\dot{\varepsilon}$ can be obtained using the energy-dissipation balance equation. The dissipation rate $\dot{\mathcal{D}}_s$ now reads

$$\dot{\mathcal{D}}_s = \int_0^\Lambda \zeta_{||} m(t) \upsilon^2 dz \simeq \frac{1}{12}\zeta_{||} m \Lambda^3 \left(\frac{\dot{\varepsilon}}{1-\phi}\right)^2 \tag{61}$$

where $\zeta_{||} = 2\pi\eta_s / k_H$ is the polymer/solvent friction constant, and *m* is the number of chains in a string cross-section. The free energy $\mathcal{F}_\Lambda$ of the string is a sum of the surface energy and the interaction energy, $\mathcal{F}_\Lambda \simeq 2\pi a \Lambda\gamma + \pi a^2 \Lambda f_{\text{int}}$, where f_{int} is defined in eq 1. Therefore, the energy-dissipation balance reads

$$\frac{d\mathcal{F}_\Lambda}{dt} \simeq -\pi a^2 \Lambda \dot{\varepsilon}\left(\frac{\gamma}{a} - \Pi\right) = -\dot{\mathcal{D}}_s \tag{62}$$

Eqs 61, 62 lead to

$$\dot{\varepsilon} = \frac{12\pi a^2 (1-\phi)^2}{m\zeta_{||}\Lambda^2}\left(\frac{\gamma}{a} - \frac{4}{\pi}\frac{T}{d^3}\phi^3\right) \tag{63}$$

Taking into account that $\dot{\varepsilon} = \dot{\phi}/\phi$, $\phi = \phi_0 a_0^2 / a^2 \ll 1$, and setting $m \approx m_0$ (m_0 is defined in eq 23), which is true since $L >> \Lambda$ (cf. also the note below eq. 66), we transform eq 63 as

$$\tau_1 d\phi / dt = \sqrt{\phi}\left[\beta - \phi^{5/2}\right], \qquad \tau_1 = \frac{\zeta_{||} d \Lambda^2}{12T} \tag{64}$$

Solving eq 64 we find the following asymptotic regimes:

$$\phi \simeq \begin{cases} \left(\dfrac{\beta t}{2\tau_1} + \sqrt{\phi_0} \right)^2, & t \ll \tau_1 / \phi_\infty^2 \\ \phi_\infty \left(1 - \exp\left(-\dfrac{5t}{2\tau_1} \beta^{4/5} \right) \right), & t \gg \tau_1 / \phi_\infty^2 \end{cases}, \tag{65a}$$

$$a \simeq \begin{cases} a_0 \left(1 + \dfrac{\beta t}{2\tau_1 \sqrt{\phi_0}} \right)^{-1}, & t \ll \tau_1 / \phi_\infty^2 \\ a_\infty \left(1 + 0.5 \exp\left(-\dfrac{5t}{2\tau_1} \beta^{4/5} \right) \right), & t \gg \tau_1 / \phi_\infty^2 \end{cases} \tag{65b}$$

Here t is the time passed since the beginning of the droplet formation.

The characteristic thinning time τ_{th} therefore is

$$\tau_{th} = \tau_1 / \phi_\infty^2 \sim \frac{\eta_s a_0^3 \phi_0}{\gamma d^2} \left(\frac{\phi_\infty}{\phi_0} \right)^{1/2} \tag{66}$$

It is longer than the linear growth time τ^* (cf. eq. 56), but shorter than the Rouse time $\tau_R \sim \tau^* (L / a_0)^2$: $\tau^* \sim \tau_{th} \sqrt{\phi_0 / \phi_\infty} \ll \tau_{th} \ll \tau_R$. Therefore, the longitudinal size of an extended polymer chain, $R_z \sim L$, changes just slightly for $t \sim \tau_{th}$ (since $\tau_{th} \ll \tau_R$). Hence $m \approx m_0$ in this regime.

The polymer chains are stretched and confined inside the Λ-strings, however, they must be somewhat swollen laterally inside the droplet regions due to repulsion of polymer segments (cf. Figure 4). The corresponding characteristic lateral size $\bar{h}$, by which the chains deviate from the straight line in the radial direction inside the droplet regions, can be estimated in analogy with the case considered above. For simplicity we consider the regime of thin strings, $a \ll a_0$. At a given chain tension $\mathcal{T}$, the bending force after deviation of the chain in the radial direction on the length $\bar{h} \ll a_0$ reads (per unit length of the chain) $f_\perp = \mathcal{T} C \sim b\mathcal{T} / a_0^2$ (the curvature in this case is $C \sim \bar{h} / a_0^2$). Polymer segments occupy the volume $\sim a_0 \bar{h}^2$ in the droplet zone ($| z | < \lambda / 2$), hence their concentration there is $c_b \sim c_0 a_0^2 / \bar{h}^2$ and the osmotic pressure equals to

$\Pi \simeq 0.5T\upsilon^* c_b^2$. The radial osmotic force $F_{osm} \sim \Pi / \bar{h} \sim T\upsilon^* c_0^2 a_0^4 / \bar{h}^5 = k_\Pi a_0^4 / \bar{h}^5$ must be compensated by the bending force $c_b l_1 f_\perp \sim 2c_0 l_1 \mathcal{T} / \bar{h}$. Therefrom we find $\bar{h} \sim a_0 \left(\frac{k_\Pi}{c_0 l_1 \mathcal{T}} \right)^{1/4}$. For $\mathcal{T} \sim T / l$ we find $\bar{h} \sim a_0 \alpha^{1/2} \ll a_0$ (cf. eq. 48), which means that the polymer swelling effect is not significant in the droplet zones (since $b \ll R$, cf. Figure 4).

To sum up, we have shown that the structure of a "beads-on-string" can appear on the final stage of thinning when the polymer chains in the thread are strongly stretched and the radius of the thread is less than the contour length of macromolecules. As mentioned in the introduction, the secondary beads-on-string structures are often observed after the elasto-capillary regime for PEO solutions.[36,54-60] A simple estimation for PEO having $M_w \sim 10^6$ g/mol (with the chain contour length $L = (M_w / M_0) l_1 \sim 10\mu\text{m}$, where $M_0 = 44$ and $l_1 \approx 0.4\text{nm}$) shows that the maximum critical radius a_0 which is found from the condition $\lambda \simeq 2\pi\sqrt{2} a_0 \le L$ should be around 1μm. The critical radius of the thread for PEO with $M_w = 4\times10^6$ g/mol found in experiment is estimated as $a_0 \approx 10$ μm[57] or even more.[54,55,59] This value is somewhat greater than that predicted by our theory ($a_0 \sim 4\mu\text{m}$). Nevertheless, the predicted fastest growing wavelength $\lambda \simeq 2\pi\sqrt{2} a_0$ is in agreement with the experiments.[56,57] This discrepancy can be explained by the existence of another mechanism, namely, the phase separation of PEO solutions caused by stretching.[62,70] The possibility of a phase separation under extension of PEO solutions had been proposed many years ago.[88] Recently, it was shown that temperature significantly affects the dynamics of thread thinning and the onset of pearling instability, which confirms the idea of phase separation.[59] In addition, computer simulations using molecular dynamics methods show that stretching of PEO oligomers in an aqueous solution leads to the formation of fibrillar structures due to a decrease in the number of hydrogen bonds between PEO and water.[89] However, it should be noted that droplet formation associated with capillary forces can still be

significant in the later stages of thread thinning since the Laplace pressure should compress the polymer core until the osmotic pressure of polymer chains stops capillary compression. The capillary mechanism of the pearling instability can be important for PAM solutions whose thinning does not depend on temperature in contrast to PEO solutions.[59] The contour length of PAM having $M_w \sim 15\times10^6$ g/mol is $L \sim 80\mu m$ ($l_1 \approx 0.4nm$), therefore the critical radius should be of order or below 8μm .

V. CONCLUDING REMARKS

We analyzed the capillary thinning dynamics of a dilute polymer solution thread for marginal or Θ solvents. Starting with a liquid bridge which tends to break in the inertial regime due to capillary forces, we focused on the thread dynamics in viscoelastic regimes where polymer chains have undergone a coil-stretch transition and a bead-on-string structure can emerge. At first, the thinning of the thread follows the well-known "inertial" law $a(t) \sim (\gamma/\rho)^{1/3}(t_b - t)^{2/3}$, where t_b is the putative breakup time. However, after a partial stretching of the chains, the viscoelastic forces begin to dominate leading to thread thinning according to a power law $a(t) \sim a_0(\tau_R / t)^2$. Such behavior differs from the exponential thinning law observed in polymer strings formed from dilute solutions. Note that our result for $a(t)$ is related to taking into account the essentially unscreened hydrodynamic interactions inherent in dilute solutions and leading to a linear dependence of the hydrodynamic friction force on chain elongation (cf. the text below eq. (4b)). Noteworthily, recent theoretical studies[48,49] on capillary thinning of dilute polymer solutions are based on a similar idea (the linear drag model[76,77]). By contrast, the friction force is proportional to the number of monomers in the case of screened hydrodynamic interactions. The latter assumption serves as a cornerstone of the theories based on the constitutive equation of Maxwell/ Oldroyd,[81] which was used, in particular, by Entov and

Hinch.[26] This famous approach predicts an exponential thinning law with constant thinning time that does not depend on concentration in the dilute solution regime. The latter prediction turns out to be in contradiction with a number of experimental and theoretical studies[35,38,42,47] on the subject (this point is further discussed below).

It is interesting to note that an additional friction mechanism related to the formation of interchain associative bonds makes it possible to explain why the exponential law is observed experimentally, rather than a power law. Such a mechanism is expected to be relevant for solutions of some polymers like PEO or polyacrylamide (PAM) in water (see section II).

Experiments involving very dilute polymer solutions also indicate a non-exponential character of thread thinning. [39,46,47] When the radius of the thread decreases down to $a_0 \sim \frac{\gamma l d^2}{\phi T}$, the chains become strongly stretched and a further thinning proceeds according to the visco-capillary law, $a(t) \sim \frac{\gamma}{6\eta}(t_b - t)$, with a strongly enhanced (renormalized) viscosity $\eta \sim \eta_s \phi N^2$. The rate of extension, $\dot{\varepsilon}(t)$, in the thinning process shows a *non-monotonic* time-dependence: it first increases as $\dot{\varepsilon} \simeq (4/3)/(t_b - t)$ in the inertial regime, but then decreases as $\dot{\varepsilon} \simeq 4/t$ in the viscoelastic regime (cf. eq. 20). Such a non-monotonic behavior of the extension rate (and, therefore, the Weissenberg number) also follows from the theory of ref. 48. It is important to note that the classical theory of exponential thinning[26] as applied to the dilute solution regime, is not entirely consistent with the experimental data.[47,48] The characteristic time τ of thinning is different from the equilibrium relaxation time τ_0, and the ratio τ/τ_0 significantly depends on concentration in the dilute regime. This dependence was explained as (partially) an effect of hydrodynamic interactions.[48]

Returning to the issue of discrepancy between the predictions given in eq. (20) and the experimental data for dilute systems, we can think of 2 other effects that can render the thinning law to become closer to an exponential decay. In the present paper we assumed the case of a

theta-solvent. However, capillary thinning was also studied for polymers in good-solvent conditions like high-molecular weight dilute solutions of polyacrylamide (PAM) in water.[33,34] The size of an unperturbed polymer coil in a dilute good-solvent regime scales as $R_0 \propto N^{\nu}$, where ν=0.6 is the Flory exponent. In this regime the tension force *f* of an elongated chain increases with the end-to-end distance *R* in a nonlinear fashion, $f \propto R^{\nu/(1-\nu)}$ for *R* << *L*. On the other hand, the polymer drag coefficient ζ_p remains proportional to *R*. What matters for the thinning law (in the viscoelastic regime) is the ratio $f/(R\zeta_p) \sim \dot{R}/R$: if it is constant (independent of *R*), an exponential thinning is predicted. If, however, this ratio decreases with *R* as $R^{-\mu}$ (here $\mu = (2-3\nu)/(1-\nu)$) a power law $a(t) \propto R^{-1/(1-\nu)} \propto t^{-1/\mu_1}$, with $\mu_1 = 2-3\nu$, is emerged. In a theta-solvent μ_1=0.5, while in good solvent μ_1=0.2, which is more than twice closer (than the theta-solvent value) to μ_1 = 0 required for the exponential thinning which would be formally predicted for ν =2/3.

The last effect concerns the molecular weight polydispersity. In the present paper we assumed a monodisperse system. In experimental systems the chains are always polydisperse, and this feature is known to be very important for polymer dynamics. This applies, in particular, to the coil-stretching kinetics during capillary thinning. In the polydisperse case shorter chains should be elongated less as they start their elongation later than chains of higher molecular weight. Moreover, as soon as the thinning rate drops at the transition to the viscoelastic regime (when the polymer stress starts to dominate the viscous stress due to the solvent), the shorter chains may start to contract thus diminishing the polymer stress and, therefore, leading to an increase of the thinning rate $\dot{\varepsilon}$ (which is opposed by the polymer stress). As a result, the effect of hydrodynamic interactions (dictating a power-law *decrease* of $\dot{\varepsilon}$, see eq. (20)) may be (at least partially) counterbalanced. As a matter of fact, the macromolecular polydispersity was taken into account in the classical study[26] showing that its effect (with no hydrodynamic

interactions) leads to a slower than exponential decrease of the filament thickness (a stretched exponential law).

To resume this part, we stress that while the single-exponential thinning law was reported in all experimental studies on dilute, semidilute and concentrated unentangled polymer solutions we know of (which is slightly surprising as such since the classical paper of Entov and Hinch[26] predicts broadening of the filament thickness decay in the case of polydisperse polymers, cf. eqs. 9, 10 in ref. 26), our theory does generically predict a power-law (t^{-2}) thinning stage due to unscreened hydrodynamic interactions in dilute theta-solutions of monodisperse high-molecular weight linear polymers in the absence of associative reversible bonds between polymer segments.

When the radius of the thread falls below a critical value a_0 which is smaller than the macromolecular contour length L, another capillary-driven instability mechanism comes into play, which is accompanied by a release of the solvent onto the thread surface in the form of annular drops. Such a mechanism has already been considered for threads of solutions of rodlike macromolecules,[71,72] where the droplet formation was found to be an activated process. By contrast, it is shown here that in threads of dilute solutions of *semi-flexible* polymers the droplet formation proceeds without any energy barrier. This leads to a fast formation of numerous annular droplets.

It is remarkable that the critical radius a_0 (cf. eq. 20) is independent of the polymer molecular weight, but is proportional to the Kuhn segment l of polymer chains, and is inversely proportional to polymer concentration, so a_0 is larger in more dilute solutions of stiffer chains. It is also important that the droplet formation time τ^* (cf. eq. 53) is much shorter than both the polymer Rouse time τ_R and the Plateau-Rayleigh time $\tau_{PR} \sim \eta a / \gamma$ of the classical capillary instability in the regime of high viscosity: the ratio $\tau_{PR} / \tau^* \sim (L / a_0)^2$ is proportional to the square of the polymer molecular weight. This property ensures that in the regime $a_0 \ll L$ the

predicted development of solvent droplets is the dominant process, possibly preventing the thread breakup and leading to fiber formation.

Thinning of polymer solution threads involving nonionic and ionic polyacrylamides of different chain rigidity in water and water/glycerol mixtures were studied experimentally in refs. 33, 34. Interestingly, both viscoelastic and quasi-Newtonian regimes (with fully stretched chains in the latter) were detected. It was found, in particular, that the ratio of the terminal elongational viscosity η_E to the corresponding relaxation time τ_E is higher for flexible (nonionic) macromolecules than for rigid-chain (ionic) samples.[34] This difference may stem from the following simple effect: the viscosity η_E is mainly defined by the total length of a stretched chain, while the relaxation time τ_E depends in addition on the chain tension; the chain tension in turn is inversely proportional to the rigidity (Kuhn) segment, so the relaxation time τ_E is directly proportional to it, hence the ratio η_E / τ_E is lower for a more rigid polymer. In addition to this effect, contact interactions between aligned rigid segments and their electrostatic interactions may play a significant role.

ACKNOWLEGEMENTS

A.V.S. acknowledges financial support from the Russian Science Foundation (Grant # 20-19-00194). A.N.S. acknowledges a partial support from the International Research Training Group (IRTG) "Soft Matter Science: Concepts for the Design of Functional Materials".

REFERENCES

(1) Denn, M. M. Continuous Drawing of Liquids to Form Fibers. *Ann. Rev. of Fluid Mech.* **1980**, 12, 365–387.

(2) Daristotle, J. L.; Behrens, A. M.; Sandler, A. D.; Kofinas, P. A Review of the Fundamental Principles and Applications of Solution Blow Spinning. *ACS Appl. Mater. Interfaces*. **2016**, 8, 34951-34963.

(3) Xue, J.; Wu, T.; Dai, Y.; Xia Y. Electrospinning and Electrospun Nanofibers: Methods, Materials, and Applications. *Chem. Rev*. **2019**, 119, 5298-5415.

(4) Malkin, A. Ya.; Petrie, C. J. S. Some conditions for rupture of polymer liquids in extension. *J. Rheol.* **1997**, 41, 1-25.

(5) McKinley, G. H. Visco-elasto-capillary thinning and break-up of complex fluids. *Rheol. Rev*. **2005**, 1-48.

(6) Malkin, A. Ya.; Arinstein, A.; Kulichikhin, V. G. Polymer extension flows and instabilities. *Progr. Polym. Si.* **2014**, 39, 959-978.

(7) Boger, D. V.; Walters, K. *Rheological Phenomena in Focus*; Elsevier Science: New York, 1993.

(8) Eggers J.; Villermaux E. Physics of liquid jets. *Rep. Prog. Phys*. **2008**, 71, 036601.

(9) Basaran, O. A. Small-Scale Free Surface Flows with Breakup: Drop Formation and Emerging Applications. *AIChE J.* **2002**, 48, 1842-1848.

(10) Chen, A. U.; Notz, P. K.; Basaran, O. A. Computational and experimental analysis of pinch-off and scaling. *Phys. Rev. Lett*. **2002**, 88, 174501.

(11) Notz, P. K.; Basaran, O. A. Dynamics and breakup of a contracting liquid filament. *J. Fluid Mech*. **2004**, 512, 223-256.

(12) Driessen, T.; Jeurissen, R.; Wijshoff, H.; Toschi, F.; Lohse, D. Stability of viscous long liquid filaments. *Phys. Fluids* **2013**, 25, 062109.

(13) Castrejón-Pita, J. R.; Castrejón-Pita, A. A.; Thete, S. S.; Sambath, K.; Hutchings, I. M.; Hinch, J.; Lister, J. R.; Basaran, O. A. Plethora of transitions during breakup of liquid filaments. *PNAS* **2015**, 112, 4582-4587.

(14) Li, Y.; Sprittles, J. E. Capillary breakup of a liquid bridge: identifying regimes and transitions. *J. Fluid Mech*. **2016**, 797, 29-59.

(15) Keller, J. B.; Miksis, M. J. Surface Tension Driven Flows. *SIAM J. Appl. Math*. 1983, 43, 268-277.

(16) Chen, Y.-J.; Steen, P. H. Dynamics of inviscid capillary breakup: collapse and pinchoff of a film bridge. *J. Fluid Mech*. **1997**, 341, 245-267.

(17) Papageorgiou, D. T. On the breakup of viscous liquid threads. *Phys. Fluids* **1995**, 7, 1529–1544.

(18) Papageorgiou, D. T. Analytical description of the breakup of liquid jets. *J. Fluid Mech*. **1995**, 301, 109-132.

(19) Lister, J. R.; Stone, H. A. Capillary breakup of a viscous thread surrounded by another viscous fluid. *Phys. Fluids* **1998**, 10, 2758-2764.

(20) Day, R. F.; Hinch, E. J.; Lister J. R. Self-Similar Capillary Pinchoff of an Inviscid Fluid. *Phys. Rev. Lett.* **1998**, 80, 704-707.

(21) Rayleigh, L. Instability of jets. *Proc. Lond. Math. Soc*. **1878**, 1, 4-13.

(22) Weber, C. Zum Zerfall eines Flussigkeitsstrahle. *ZAMM* **1931**, 11, 136-154.

(23) Bazilevskii, A. V.; Voronkov, S.I.; Entov, V.M.; Rozhkov, A.N. Orientation effects in the breakup of jets and threads of dilute polymer solutions. *Sov. Phys. Dokl.*, **1981**, 26, 333-336.

(24) Bazilevskii, A.V.; Entov, V. M.; Lerner, M. M.; Rozhkov A. N. Failure of polymer solution filaments. *Polym. Sci. Ser. A*. **1997**, 39, 316-324.

(25) Yarin, A. L. *Free liquid jets and films: hydrodynamics and rheology*; John Wiley & Sons: New York, 1993.

(26) Entov, V.M.; Hinch E.J. Effect of a spectrum of relaxation times on the capillary thinning of a filament of elastic liquid. *J. Non-Newtonian Fluid Mech*. **1997**, 72, 31–53.

(27) Amarouchene, Y.; Bonn, D.; Meunier, J.; Kellay, H. Inhibition of the Finite-Time Singularity during Droplet Fission of a Polymeric Fluid. *Phys. Rev. Lett.* **2001**, 86, 3558-3561.

(28) Deblais, A; Herrada, M. A.; Eggers, J.; Bonn D. Self-similarity in the breakup of very dilute viscoelastic solutions. *J. Fluid Mech.* **2020**, 904, R2.

(29) Chang, H.-C.; Demekhin, E. A.; Kalaidin, E. Iterated stretching of viscoelastic jets. *Phys. Fluids* **1999**, 11, 1717-1737.

(30) Li, J.; Fontelos, M. A. Drop dynamics on the beads-on-string structure for viscoelastic jets: A numerical study. *Phys. Fluids* **2003**, 15, 922-937.

(31) Bhat, P. P.; Basaran, O. A.; Pasquali, M. Dynamics of viscoelastic liquid filaments: Low capillary number flows. *J. Non-Newtonian Fluid Mech*. **2008**, 150, 211-225.

(32) Bhat, P. P.; Appathurai, S.; Harris, M. T.; Pasquali, M.; McKinley, G. H.; Basaran, O. A. Formation of beads-on-a-string structures during break-up of viscoelastic filaments. *Nat. Phys*. **2010**, 6, 625-631.

(33) Stelter, M.; Brenn, G.; Yarin, A. L.; Singh, R. P.; Durst F. Validation and application of a novel elongational device for polymer solutions. *J. Rheol*. **2000**, 44, 595-616.

(34) Stelter, M.; Brenn, G.; Yarin, A. L.; Singh, R. P.; Durst F. Investigation of the elongational behavior of polymer solutions by means of an elongational rheometer. *J. Rheol*. **2002**, 46, 507-527.

(35) Bazilevskii, A. V.; Entov, V. M.; Rozhkov A. N., Breakup of an Oldroyd liquid bridge as a method for testing the rheological properties of polymer solutions, *Polym. Sci., Ser. A Ser. B* **2001**, 43, 716-726.

(36) Christanti, Y.; Walker, L. M. Surface tension driven jet break up of strain-hardening polymer solutions. *J. Non-Newtonian Fluid Mech.* **2001**, 100, 9-26.

(37) Clasen, C.; Eggers, J.; Fontelos, M. A.; Li, J.; McKinley, G. H. The beads-on-string structure of viscoelastic threads. *J. Fluid Mech*. **2006**, 556, 283-308.

(38) Tirtaatmadja, V.; McKinley, G. H.; Cooper-White, J. J. Drop formation and breakup of low viscosity elastic fluids: Effects of molecular weight and concentration. *Phys. Fluids*, **2006**, 18, 043101.

(39) Dinic, J.; Zhang, Y.; Jimenez L. N.; Sharma, V. Extensional Relaxation Time of Dilute, Aqueous, Polymer Solutions. *ACS Macro Lett.* **2015**, 4, 804-808.

(40) Dinic, J.; Jimenez L. N.; Sharma, V. Pinch-off dynamics and dripping-onto-substrate (DoS) rheometry of complex fluids. *Lab Chip*. **2017**, 17, 460-473.

(41) Jimenez L. N.; Dinic, J.; Parsi, N.; Sharma, V. Extensional Relaxation Time, Pinch-Off Dynamics, and Printability of Semidilute Polyelectrolyte Solutions. *Macromolecules* **2018**, 51, 5191-5208.

(42) Dinic, J.; Sharma, V. Macromolecular relaxation, strain, and extensibility determine elastocapillary thinning and extensional viscosity of polymer solutions. *PNAS* **2019**, 116, 8766–8774.

(43) Keshavarz, B.; Sharma, V.; Houze, E. C.; Koerner, M. R.; Moore, J. R.; Cotts, P. M.; Threlfall-Holmes, P.; McKinley, G. H. Studying the effects of elongational properties on atomization of weakly viscoelastic solutions using Rayleigh Ohnesorge Jetting Extensional Rheometry (ROJER). *J. Non-Newtonian Fluid Mech*. **2015**, 222, 171–189.

(44) Mathues, W.; Formenti, S.; McIlroy, C.; Harlen, O. G.; Clasen C. CaBER vs ROJER - Different time scales for the thinning of a weakly elastic jet. *J. Rheol*. **2018**, 62, 1135-1153.

(45) Mackley, M. R.; Butler, S. A.; Huxley, S.; Reis, N. M.; Barbosa, A. I.; Tembely, M. The observation and evaluation of extensional filament deformation and breakup profiles for Non Newtonian fluids using a high strain rate double piston apparatus. *J. Non-Newtonian Fluid Mech*. **2017**, 239, 13–27.

(46) Sur, S.; Rothstein, J. Drop breakup dynamics of dilute polymer solutions: Effect of molecular weight, concentration, and viscosity. *J. Rheol*. **2018**, 62, 1245-1259.

(47) Clasen, C.; Plog, J.P.; Kulicke, W.-M.;Owens, M.; Macosko, C.; Scriven, L.E.;Verani, M.; McKinley, G.H. How dilute are dilute solutions in extensional flows? *J. Rheol*. **2006**, 50, 849-881.

(48) Prabhakar, R.; Gadkari, S.; Gopesh, T.; Shaw, M. J. Influence of stretching induced self-concentration and self-dilution on coil-stretch hysteresis and capillary thinning of unentangled polymer solutions. *J. Rheol*. **2016**, 60, 345-366.

(49) Prabhakar, R.; Sasmal, C.; Nguyen, D. A.; Sridhar, T.; Prakash, J. R. Effect of stretching-induced changes in hydrodynamic screening on coil-stretch hysteresis of unentangled polymer solutions. *Phys. Rev. Fluids*. **2017**, 2, 011301(R).

(50) Anna, S. L.; McKinley, G. H. Elasto-capillary thinning and breakup of model elastic liquids. *J. Rheol*. **2001**, 45, 115-138.

(51) Mora, S.; Phou, T.; Fromental, J.M.; Pismen, L.M.; Pomeau, Y. Capillarity driven instability of a soft solid. *Phys. Rev. Lett.* **2010**, 105, 214301.

(52) Snoeijer, J.H.; Pandey, A.; Herrada, M.A.; Eggers, J. The relationship between viscoelasticity and elasticity. *Proc. Roy. Soc. A* **2020**, 476, 20200419.

(53) Pandey, A.; Kansal, M.; Herrada, M.A.; Eggers, J.; Snoeijer, J.H. Elastic Rayleigh–Plateau instability: dynamical selection of nonlinear states. *Soft Matter* **2021**,17, 5148-5161.

(54) Oliveira, M. S. N.; McKinley, G. H. Iterated stretching and multiple beads-on-a-string phenomena in dilute solutions of highly extensible flexible polymers. *Phys. Fluids* **2005**, 17, 071704.

(55) Oliveira, M. S. N.; Yeh, R.; McKinley, G. H. Iterated stretching, extensional rheology and formation of beads-on-a-string structures in polymer solution. *J. Non-Newtonian Fluid Mech*. **2006**, 137, 137–148.

(56) Sattler, R.; Wagner, C.; Eggers, J. Blistering Pattern and Formation of Nanofibers in Capillary Thinning of Polymer Solutions. *Phys. Rev. Lett*. **2008**, 100, 164502.

(57) Sattler, R.; Gier, S.; Eggers, J.; Wagner, C. The final stages of capillary break-up of polymer solutions. *Phys. Fluids* **2012**, 24, 023101.

(58) Bazilevskii, A.V.; Rozhkov A. N. Dynamics of the Capillary Breakup of a Bridge in an Elastic Fluid. *Fluid Dynamics*. **2015**, 50, 800-811.

(59) Deblais, A., K. P. Velikov, and D. Bonn, Pearling Instabilities of a Viscoelastic Thread, *Phys. Rev. Lett*. **2018**, 120, 194501.

(60) Kibbelaar, H. V. M.; Deblais, A.; Burla, F.; Koenderink, G. H.; Velikov, K. P.; Bonn, D. Capillary thinning of elastic and viscoelastic threads: From elastocapillarity to phase separation. *Phys. Rev. Fluids*. **2020**, 5, 092001(R).

(61) Semakov, A. V.; Kulichikhin, V. G.; Tereshin, A. K.; Antonov, S. V.; Malkin, A. Ya. On the nature of phase separation of polymer solutions at high extension rates. *J. Polym. Sci. B: Phys Ed.* **2015**, 53, 559-565.

(62) Malkin, A. Ya.; Semakov, A. V.; Skvortsov, I. Yu.; Zatonskikh, P.; Kulichikhin, V. G.; Subbotin, A. V.; Semenov, A. N. Spinnability of Dilute Polymer Solutions. *Macromolecules* **2017**, 50, 8231-8244.

(63) Kulichikhin, V. G.; Skvortsov, I. Yu.; Subbotin, A. V.; Kotomin, S. V.; Malkin, A. Ya. A novel technique for fiber formation: Mechanotropic spinning - principle and realization. *Polymers* **2018**, 10, 856.

(64) Eggers, J. Instability of a polymeric thread. *Phys. Fluids* **2014**, 26, 033106.

(65) Helfand, E.; Fredrickson, G. H. Large fluctuations in polymer solutions under shear. *Phys. Rev. Lett.* **1989**, 62, 2468-2471.

(66) Doi, M.; Onuki, A. Dynamic coupling between stress and composition in polymer solutions and blends. *J. Phys. II France* **1992**, 2, 1631-1656.

(67) Milner, S. T. Dynamical theory of concentration fluctuations in polymer solutions under shear. *Phys. Rev. E* **1993**, 48, 3674-3691.

(68) Subbotin, A. V.; Semenov, A. N. Phase Separation in Dilute Polymer Solutions at High-Rate Extension. *J. Polym. Sci.: Part B: Phys Ed.* **2016**, 54, 1066-1073.

(69) Semenov, A. N.; Subbotin, A. V. Phase Separation Kinetics in Unentangled Polymer Solutions Under High-Rate Extension. *J. Polym. Sci.: Part B: Phys Ed.* **2017**, 55, 623-637.

(70) Subbotin, A. V.; Semenov, A. N. Phase Separation in Polymer Solutions under Extension. *Polym. Sci. C* **2018**, 60, S106-S117.

(71) Subbotin, A. V.; Semenov, A. N. Capillary-induced Phase Separation in Ultrathin Jets of Rigid-chain Polymer Solutions. *JETP Lett* **2020**, 111, 55–61.

(72) Subbotin, A. V.; Semenov, A. N. Multiple droplets formation in ultrathin bridges of rigid rod dispersions. *J. Rheol.* **2020**, 64, 13-27.

(73) Rubinstein, M.; Colby, R. *Polymer Physics*, Oxford: New York, 2003.

(74) Semenov, A. N.; Khokhlov, A. R. Statistical physics of liquid-crystalline polymers. *Phys. Usp.* **1988**, 156, 988-1014.

(75) de Gennes, P.G. *Scaling Concepts in Polymer Physics*; Cornell Univ. Press: Ithaca, 1979.

(76) Hinch, E. J. Mechanical models of dilute polymer-solutions in strong flows, *Phys. Fluids* **1977**, 20, S22–S30.

(77) Dunlap, P. N.; and Leal, L. G. Dilute polystyrene solutions in extensional flows: birefringence and flow modification, *J. Non-Newtonian Fluid Mech*. **1987**, 23, 5–48.

(78) Pincus P. Excluded Volume Effects and Stretched Polymer Chains. *Macromolecules* **1976**, 9, 386-388.

(79) Doi, M.; Edwards, S. F. *The Theory of Polymer Dynamics*; Oxford Univ. Press: New York, 1986.

(80) This equation for k_H is valid for $s \sim 1$. In the general case (including $s << 1$) the equation should be modified as $k_H \simeq 0.5\ln(s/\phi) - (1-s)\ln(l/d)$. The weak dependence of k_H on s is neglected in what follows.

(81) Bird, R.B.; Armstrong, R.C.; Hassager, O. *Dynamics of Polymeric Fluids*; Wiley: New York, 1987.

(82) Larson, R. G. The unraveling of a polymer chain in a strong extensional flow. *Rheol. Acta* **1990**, 29, 371-384.

(83) McKinley, G. H.; Tripathi, A. How to extract the Newtonian viscosity from capillary breakup measurements in a filament rheometer. *J. Rheol*. **2000**, 44, 653-670.

(84) Rubinstein, M.; Semenov, A.N. Thermoreversible gelation in solutions of associating polymers: 2. Linear dynamics. *Macromolecules* **1998**, 31, 1386-1397.

(85) Ho, D. L.; Hammouda, B.; Kline, S. R. Clustering of Poly(ethylene oxide) in Water Revisited. *J. Polym. Sci.: Part B: Phys Ed.* **2003**, 41, 135–138.

(86) Hammouda, B.; Ho, D. L.; Kline, S. R. SANS from Poly(ethylene oxide)/Water Systems. *Macromolecules* **2002**, 35, 8578-8585.

(87) James D. F.; Saringer J. H. Extensional flow of dilute polymer solutions. *J. Fluid Mech.* **1980**, 97, 666-671.

(88) Ferguson, J.; Hudson, N.E.; Warren, B.C.H. Structural changes during elongation of polymer solutions, *J. Non-Newtonian Fluid Mech.* **1987**, 23, 49-72.

(89) Donets, S; Sommer J.-U. Molecular Dynamics Simulations of Strain-Induced Phase Transition of Poly(ethylene oxide) in Water. *J. Phys. Chem. B* **2018**, 122, 392 - 397.